Chinese Chemical Letters 35 (2024) 108420

Contents lists available at ScienceDirect

Chinese Chemical Letters

journal homepage: www.elsevier.com/locate/cclet

Preparation of multicolor carbon dots with thermally turn-on fluorescence for multidimensional information encryption

Chan Wang[a,*], Jianfeng Huang[b], Yimin He[a], Guoxia Ran[a], Qijun Song[a,*]

[a] Key Laboratory of Synthetic and Biological Colloids, Ministry of Education, International Joint Research Center for Photoresponsive Molecules and Materials, School of Chemical & Material Engineering, Jiangnan University, Wuxi 214122, China
[b] Department of Radiation Oncology, Affiliated Hospital of Jiangnan University, Wuxi 214122, China

ARTICLE INFO

Article history:
Received 6 February 2023
Revised 30 March 2023
Accepted 31 March 2023
Available online 5 April 2023

Keywords:
Carbon dots
Precursor-oriented structure
Full-color fluorescence
Turn-on thermosensitivity
Advanced anti-counterfeiting

ABSTRACT

Carbon dots (CDs) with superior fluorescence properties have attracted a growing number of research interests in anti-counterfeiting. However, the preparation of CDs with thermally turn-on fluorescence and full-color-emitting in visible spectrum is still a big challenge due to the complicated reaction mechanism in the formation of CDs. Here, a simple precursor-oriented strategy for the preparation of multicolor CDs with heat-stimuli turn-on fluorescence is reported. Comprehensive experimental characterizations and theoretical calculations revealed that the emission wavelength of CDs can be readily tuned from 460 nm to 654 nm with selected precursors, which was ascribed to the extent of conjugated sp^2-domains (core states) and the amount of oxygen- and nitrogen-containing groups bound to sp^2-domains (surface states). After simply mixing two or three kinds of CDs, a full-color range of fluorescence emission was realized, and the CDs-based fluorescence inks were successfully fabricated. Particularly, all the printed patterns from the inkjet exhibited a thermal-induced enhancement in fluorescence. On this basis, combining CDs with heating-induced "turn-off" fluorescence materials can lead to multidimensional and multistage encryption. These results demonstrate that the thermochromic and photochromic CDs with much more enhanced security exhibit promising application in data storage and encryption.

Information security is an ever-growing global hotspot that is urgently required not only in economic and military fields but also in our daily life. Much effort has been continuously devoted to develop advanced encryption strategies in information protection and data security [1–4]. In recent years, various types of smart materials and approaches for encryption have been reported. Especially stimuli-responsive fluorescence materials that can implement the data encryption by their changeable and reversible luminescence behaviors have received extensive investigations [5,6]. According to the external stimuli, these materials can be classified into thermochromic, mechanochromic, solvochromic and electrochromic [7–10]. Owing to the easiness of being copied and counterfeited of single-level anti-counterfeiting materials, it is of great importance for developing functional fluorescence materials with the performance of multidimensional and multistage encryption.

Carbon dots (CDs) are an emerging kind of metal-free carbon nanomaterials with remarkable characteristics of tunable photoluminescence (PL), good solubility, high photostability and diverse synthetic methods [11–14]. These intrinsic advantages endow CDs an attractive candidate for anti-counterfeiting and information encryption [15,16]. For example, Jiang *et al*. reported a triple-mode emission of CDs that simultaneously exhibited photoluminescence, up-conversion photoluminescence and phosphorescence [17]. Ren *et al*. prepared a type of CDs with time-dependent phosphorescence color by hydrothermal treatment of levofloxacin, and the resulting CDs were applied in dynamic phosphorescence colored three dimensional (3D) codes for information encryption [18]. Shi *et al*. confined CDs in the interlayers of layered double hydroxides to obtain an ensemble that possessed dual-emission of fluorescence and room temperature phosphorescence properties, which provided a high level of security against counterfeiting [19]. However, these CDs still belong to single stimuli (light) PL materials, and their PL is often quenched by external stimuli (*e.g.* heat, pressure, metal ions, pH, moisture and chemical reagents), which limit their practical use in anti-counterfeiting [20–22]. Hence the development of advanced CDs that can possess stimuli turn-on PL is urgently required.

* Corresponding authors.
E-mail addresses: wangchan@jiangnan.edu.cn (C. Wang), qsong@jiangnan.edu.cn (Q. Song).

https://doi.org/10.1016/j.cclet.2023.108420
1001-8417/

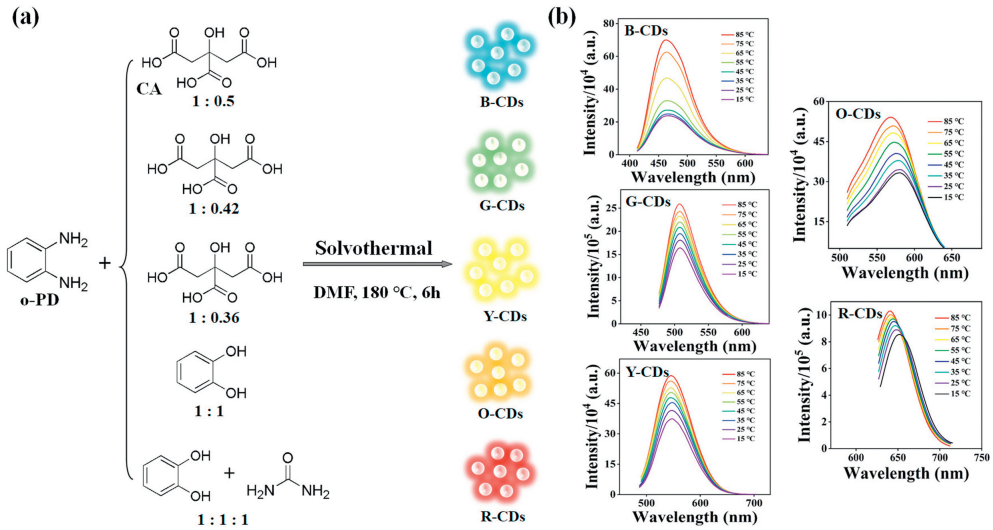

Fig. 1. (a) A precursor-oriented strategy for synthesis of CDs with multiple color emission using solvothermal method. (b) Fluorescence spectra of five CDs in aqueous solution with turn-on thermochromic characteristics.

In our previous work, we have prepared a series of thermally turn-on fluorescence CDs that provide strong anti-interference capability and enhanced spatial resolution [23,24]. Ideally the heat stimuli can be generated by the human body temperature, a hair dryer or lighter without the need of sophisticated instruments or laboratory environment, thereby providing a convenient operation with high reliability. To achieve multilevel encrypting data more effectively, multicolor CDs with turn-on thermochromic characteristics are developed for the first time in this work. Although multicolor CDs have been extensively studied in recent years [25–29], however, full color CDs with thermally turn-on fluorescence have not been reported so far. Therefore, it is necessary to develop a convenient method to tune the emission of turn-on thermosensitive CDs in advanced anti-counterfeiting. Herein the color-tunable emission properties were achieved by scrutinizing selection of precursors. Subsequent characterizations reveal that the CDs with blue, green, yellow, orange or red colors are caused by increasing size of conjugated domains and amount of carbonyl and amino groups. These characteristics are in line with those of selected precursors, suggesting the structures of precursors are partially preserved in the resultant CDs. By simply mixing different kinds of CDs, the composite CDs with bright and remarkably stable full-color and white light can be obtained. The full color fluorescence inks for inkjet printing were also prepared from these composite CDs, and they were successfully applied for the anti-counterfeiting of real samples. All the printed patterns, including quick response (QR) codes, colorful numbers and “tiger” logo, can vividly appear on the printed paper with very fine details. In view of the thermal-induced enhancement in fluorescence for resulting CDs, visible fluorescence color evolution with a high contrast and clear signal can be provided by combining CDs with the heat-quenching fluorescence. Our method elicits an advanced anti-counterfeiting strategy that creates high-quality features with a multilevel encryption by multicolor emissions coupled with thermochromic characteristics.

Compared with small molecules such as citric acid and urea, the precursors containing multiple aromatic ring and heteroatoms were used to fabricate multicolor CDs, which can avoid the complicated polymerization process. Thus, a simple precursor-oriented method was adopted in this work for tuning the emission of CDs by partially retaining the characteristic structures of precursors. As shown in Fig. 1a, the CDs are prepared by solvothermal reaction in *N*,*N*-dimethylformamide at 180 °C for 6 h, and the multiple color emissive CDs were readily produced by tuning the amounts of precursors. *o*-Phenylenediamine (o-PD) is considered as the main precursor, and the blue emissive CDs (B-CDs) can be obtained when o-PD and citric acid (CA) were selected as precursors. With the increase of the o-PD content, the green and yellow emissive CDs (G-CDs and Y-CDs) are obtained. Unlike CA, catechol is known as an aromatic compound with conjugated structures, and the orange emissive CDs (O-CDs) are prepared when o-PD and catechol are used as precursors. Furthermore, the introduction of nitrogen-containing precursor (urea), the maximum emission of the resulting CDs (R-CDs) shifts to red light. Thus, the tunable emission of CDs can be realized by simply selecting the precursors with difference in conjugated structure and nitrogen-containing groups. The fluorescence spectra of CDs show the emission peaks cover the entire visible spectrum. More importantly, these multicolor CDs exhibit enhanced responses to temperature increments (Fig. 1b). According to the equation [23,24], thermal sensitivities (S) for B-CDs, G-CDs, Y-CDs, O-CDs and R-CDs solutions are calculated as 2.77%/°C, 0.82%/°C, 0.81%/°C, 0.63%/°C and 0.29%/°C, respectively. The good linear relationships between fluorescence intensity and temperature with the correlation coefficient (R^2) of 0.99–0.999 are obtained as shown in Fig. S1 (Supporting information). According to our previous work, it is considered that the precursor-dependent intramolecular hydrogen bonds (IHBs) determined the thermal sensitivity of target CDs [23,24]. The differential scanning calorimetry (DSC) measurements in Fig. S2 (Supporting information) demonstrate that the endothermic transitions of five CDs are before 100 °C, which may be attributed to the presence of IHBs [30–32]. Thus, the difference in the thermal sensitivity of obtained five CDs may be also caused by the selected precursors.

The ultraviolet–visible (UV–vis) absorption spectra in Fig. S3 (Supporting information) display the absorption behaviors of the multicolor CDs, and the subtle differences in absorption of the five CDs indicate their structural discrepancies. As shown in the inset of Fig. S3, all CDs exhibit good dispersion in aqueous solution, and their emissions exhibit strongly bright under UV light irradiation. Furthermore, the maximum emission peaks for these CDs are independent of the excitation wavelength (Fig. S4 in Supporting information), suggesting the CDs have a uniform size distribution and a single PL center. The time-resolved photoluminescence decay spectra of CDs were measured (Fig. S5a and Table S1 in Supporting information), and the average lifetimes (τ_a) of B-CDs, G-CDs, Y-CDs, O-CDs and R-CDs are 5.96, 5.26, 4.46, 2.43 and 2.15 ns, respectively. The decrease of τ_a indicates the increase in the nonradiative traps

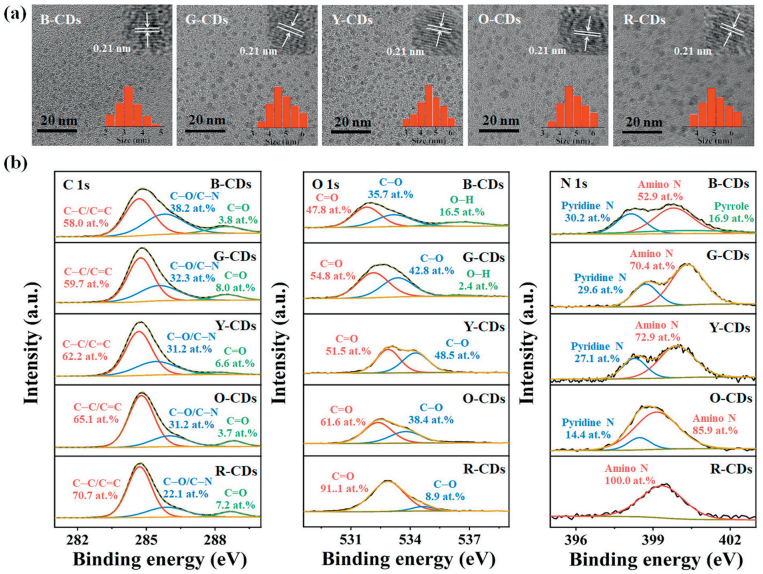

Fig. 2. (a) TEM images of the B-CDs, G-CDs, Y-CDs, O-CDs and R-CDs; inset: HRTEM images (top) and size distribution (bottom). (b) High-resolution C 1s, O 1s and N 1s XPS spectra for multicolor emissive CDs.

as the increased degree of carbonization, thereby red-shifting the PL wavelengths. And this trend corresponds to the variation of absolute quantum yields (QYs). Here, the τ_a values of all CDs have shown little variation with temperature (Figs. S5b–f in Supporting information), which is very different from the normal PL properties that usually exhibit attenuated fluorescence intensities and τ_a as the temperature increases. This peculiarity originated from IHBs-regulated chromophore structures in CDs, as it has been confirmed in our previous work [23,24].

The transmission electron microscope (TEM) images (Fig. 2a) illustrate the as-prepared CDs are quasi-spherical and uniform monodisperse particles with average diameters of 3.5 nm (B-CDs), 4.2 nm (G-CDs), 4.5 nm (Y-CDs), 4.8 nm (O-CDs) and 5.1 nm (R-CDs). The high-resolution TEM (HRTEM) images demonstrate that all CDs have well-resolved lattice fringes with a spacing of 0.21 nm, which can be ascribed to (100) crystal plane of graphitic carbon [33,34]. The dynamic light scattering (DLS) analysis in Fig. S6 (Supporting information) demonstrates that the average sizes of CDs are in the range of 50–80 nm, which are much larger than those of CDs that observed in the TEM images (Fig. 2), suggesting the expansion of polymer chains on the surface of CDs in solution [23,35,36]. And the changes in hydrated radius of multicolor CDs are consistent with the results of TEM analyses, suggesting that the actual particle sizes may have a great influence on the optical behavior of CDs. The full-survey X-ray photoelectron spectroscopy (XPS) spectra (Fig. S7 in Supporting information) exhibit that all CDs are composed of C, O and N elements, and their atomic ratios were provided in Table S2 (Supporting information). The content of nitrogen atoms in CDs increases with the red shift of emission wavelength, which agrees well with the change in nitrogen content of precursors. A similar trend can be observed in high-resolution C 1s spectra (Fig. 2b and Table S3 in Supporting information) where the sp^2 carbon atoms (C=C/C–C) at 284.8 eV in the region typical for sp^2-hybridized domains increase as the emission of CDs red shifts [37,38]. It means that the selection for special precursors with extended sp^2 domains and increased N content is particularly useful to obtain CDs with long wavelength. The O 1s XPS spectra show the difference in five CDs, where three components are associated with –OH at 536.4 eV, C–O at 534.3 eV and C=O at 531.7 eV in B-CDs and G-CDs, while only C–O and C=O bonds can be observed in Y-CDs, O-CDs and R-CDs. As shown in Table S4 (Supporting information), the relative amount of C=O bonds, corresponding to the degree of oxidation, increases with the red-shifting emission of CDs [39,40]. More details can be observed in the N 1s spectra that three component peaks of N 1s bands at 398.6, 399.7 and 401.2 eV represent pyridinic N, amino N and pyrrolic N, respectively [41,42]. From B-CDs to R-CDs (Table S5 in Supporting information), the content of electron-donating NH_2 groups increases, which can cause the decreased band gap energy and the redshifted emission wavelength. Furthermore, the results of the Fourier transform infrared spectra (Fig. S8 in Supporting information) are in full accordance with XPS data. The characteristic absorption peak in the R-CDs located at about 1500 cm^{-1} originates from the stretching vibrations of C=C bonds [36,43,44]. Based on the above analyses, the increase in conjugated domains with the nitrogen/oxygen-related surface defects of CDs leads to the red-shifted PL.

Although all CDs exhibit the single PL center, the structure of chromophores in resulting CDs are different according to the above results. Thus, we further investigated the fluorescence mechanism of the multicolor-emissive CDs by density functional theory (DFT) calculations. The CDs are generally considered to be composed of sp^3/sp^2-hybridized carbon cores with different surface groups [27,45-47]. Here several sp^3/sp^2-hybridized benzene ring structures as the possible models were proposed to assess the synergistic effect of sp^2 domains size and oxygen-/nitrogen-related surface states on the fluorescence emission of CDs (Fig. 3). The corresponding energy of the band gap (E_g), highest occupied molecular orbital (HOMO) and lowest unoccupied molecular orbital (LUMO) were estimated by theoretical calculations. Obviously, the E_g values of five models were close to the experimental data, which can be calculated from the UV–vis diffuse reflectance spectra (Fig. S9 in Supporting information). As expected, the increase in the size of sp^2 domains and the amount of oxygen- and nitrogen-related functional groups would lower the E_g and cause the red-shift emission wavelength. Hence, the enhanced graphitization degree and structural defects of CDs play vital roles in the decrease of E_g.

We further evaluated the practical use of resulting CDs for anti-counterfeiting purpose. A series of fluorescence inks was initially prepared by mixing CDs with different mass ratio and type, and 36-color mixtures with different fluorescence were successfully obtained, then brush-coated on A4 papers. As shown in Fig. 4a, all the patterns with bright fluorescence are clearly visible under

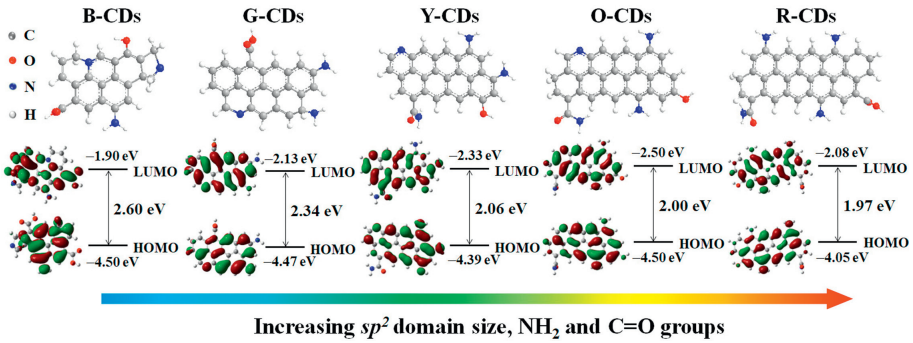

Fig. 3. Schematic illustration of the multicolor emission from CDs by DFT analysis for the structural models. Optimized models are composed of 6 to 8 polyaromatic rings with substituents locating at different sites, and their calculated HOMO and LUMO energy levels are listed below.

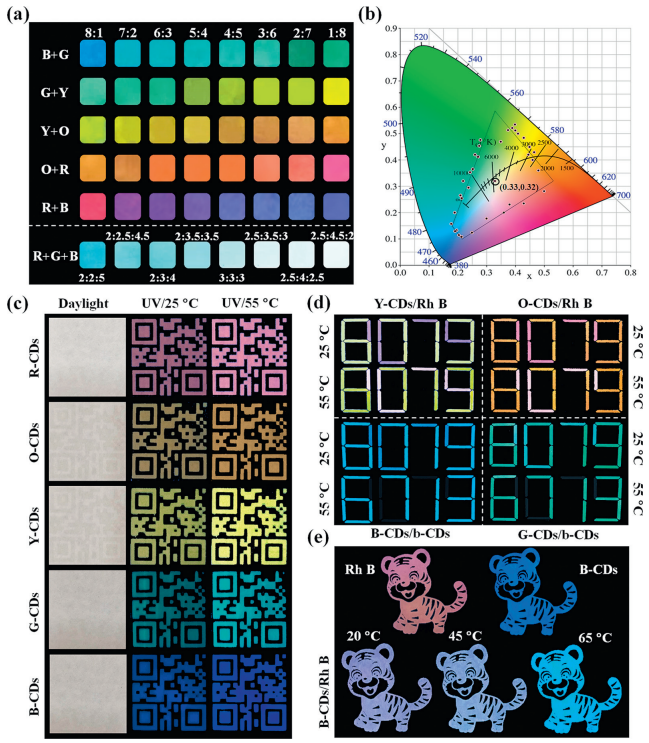

Fig. 4. (a) Patterns with the full-color display on A4 paper are generated by adjusting the mix type and mass ratio of CDs under UV light. (b) CIE chromaticity coordinates of hybrid CDs. The letters of "B", "G", "Y", "O" and "R" represent the B-CDs, G-CDs, Y-CDs, O-CDs and R-CDs. (c) QR code encryption by multicolor CDs; left: photos under daylight, middle: photos taken at room temperature under UV light, right: photos taken at 55 °C under UV light. (d) Security number coding encryption of "8079" at different temperature by multicolor CDs; the numbers "6713" were printed by Y-CDs, O-CDs, B-CDs and G-CDs, respectively, and the corresponding rest were printed by Rh B (top) and b-CDs (bottom). (e) Image printing; optical photos of "tiger" patterns by B-CDs, Rh B and their mixture at different temperatures.

UV light. And the coordinates of the fluorescence of all hybrid CDs marked on the Commission International de L'Eclairage (CIE) chromaticity diagram cover most of the visible light region from 400 nm to 780 nm (Fig. 4b). The more detailed values of CIE coordinates are provided in Table S6 (Supporting information). Furthermore, the white emissive hybrid CDs can be obtained by simply blending the three chromic components (R-CDs, G-CDs and B-CDs) at a mass ratio of 2.5:4.5:2, and the corresponding CIE coordinate appears at (0.33, 0.32), which is close to that of pure white light (0.33, 0.33), indicating the good white-light performance. Highly luminescent CDs-based inks with multicolor and white light emission were successfully synthesized, and these color-switchable fluorescence properties of CDs by arranging them in distinct combination and sequence endow the related information encryption with great complexity, demonstrating a promising prospect in anti-counterfeiting.

We also filled the standard ink cartridges with the corresponding CDs in a commercially available desktop inkjet printer (Canon MG2580S). As shown in Fig. 4c, the quick response (QR) codes were printed with the fluorescent inks. Under UV light irradiation, these codes exhibit blue, green, yellow, orange and red emission, respectively, and the complete encoded information could be clearly and accurately recognized by the naked eye. Their fluorescence becomes stronger as the temperature increases compared with those at room temperature, and this heat-induced "light-on" fluorescence behavior displays enhanced thermal sensitivity, which offers the second mode of anti-counterfeiting. In addition, the "light-on" CDs together with "turn-off" properties of fluorescence materials (*i.e.* Rh B and a blue emissive CDs (b-CDs)) are used to make forgers more difficult to counterfeit. As exhibited in Fig. 4d, the "8079" codes with two parts were printed on A4 papers, where the "6713" codes were separately printed by four "light-on" fluorescent inks, and the remain regions were printed by Rh B (top) and b-CDs (bottom), respectively. After exposing the printed paper at 55 °C, the fluorescence intensity of "6713" codes enhance, and thus the color of this part is brighter. In contrast, the fluorescence intensity of Rh B becomes weaken at high temperature, and the b-CDs fluorescence is completely quenched at 55 °C, causing the number of "8079" turns to "6713". As expected, these color changes are easily distinguishable, consequently providing the third layer of security. Furthermore, we loaded three CDs inks (Rh B, b-CDs and their mixture) into the ink cartridges, and then printed the pattern "tiger", which shows distinctly different fluorescence at different temperature. Such visible evolution of fluorescence color provides much higher contrast and clearer signals with more difficult in replication compared with the change of fluorescence intensity, demonstrating a great application prospect in advanced anti-counterfeiting.

We proposed a simple precursor-dependent strategy to synthesize turn-on thermosensitive CDs with multicolor emission. Detailed structural and optical characterizations together with theoretical calculations revealed that the red-shift emission of CDs can be attributed to the increase in size of sp^2 domains and content of C=O and NH_2 groups. The CDs-based fluorescence inks with full-color emission were obtained by mixing two or three kinds of CDs, which can be conveniently applied in the computerized inkjet printing. The printed patterns displayed reversible color-changing behaviors under the stimulation of heat and irradiation light. In addition, these turn-on thermosensitive CDs were incorporated with the heating-quenching fluorescence material to pro-

duce complicated patterns with enhanced counterfeiting capability. The results obtained in this work could inspire the development of thermochromic and photochromic CDs for advanced information encryption, and further build a new way for the exploration of novel anti-counterfeiting technologies.

Declaration of competing interest

The authors declare that they have no known competing financial interests or personal relationships that could have appeared to influence the work reported in this paper.

Acknowledgments

This work is supported by the Natural National Science Foundation of China (No. 51973083), the Fundamental Research Funds for the Central Universities (No. JUSRP22027), and clinical research and translational medicine program of affiliated hospital of Jiangnan University (No. LCYJ202239). Dr. Chan Wang would like to acknowledge the work of the Central Laboratory, School of Chemical and Material Engineering, Jiangnan University.

Supplementary materials

Supplementary material associated with this article can be found, in the online version, at doi:10.1016/j.cclet.2023.108420.

References

[1] R. Arppe, T.J. Sørensen, Nat. Chem. Rev. 1 (2017) 0031.
[2] X. Hou, C. Ke, C.J. Bruns, et al., Nat. Commun. 6 (2015) 6884.
[3] J. Andréasson, U. Pischel, Chem. Soc. Rev. 47 (2018) 2266–2279.
[4] Y. Zhang, M. Li, S. Lu, Small 19 (2022) 2206080.
[5] W. Ren, G. Lin, C. Clarke, et al., Adv. Mater. 32 (2020) 1901430.
[6] X. Yu, H. Zhang, J. Yu, Aggregate 2 (2021) 20–34.
[7] X. Duan, S. Kamin, N. Liu, Nat. Commun. 8 (2017) 14606.
[8] W. Huang, M. Xu, J. Liu, et al., Adv. Func. Mater. 29 (2019) 1808762.
[9] Z. Liu, H.K. Bisoyi, Y. Huang, et al., Angew. Chem. Int. Ed. 61 (2022) 202115755.
[10] Y. Ru, B. Zhang, X. Yong, et al., Adv. Mater. 35 (2023) 2207265.
[11] J. Liu, R. Li, B. Yang, ACS Cent. Sci. 6 (2020) 2179–2195.
[12] F. Arcudi, L. Đorđević, M. Prato, Acc. Chem. Res. 52 (2019) 2070–2079.
[13] L. Ai, Z. Song, M. Nie, et al., Angew. Chem. Int. Ed. 62 (2023) e202217822.
[14] W. Li, Y. Liu, B. Wang, et al., Chin. Chem. Lett. 30 (2019) 2323–2327.
[15] X. Yang, X. Li, B. Wang, et al., Chin. Chem. Lett. 33 (2022) 613–625.
[16] X. Niu, T. Song, H. Xiong, Chin. Chem. Lett. 32 (2021) 1953–1956.
[17] K. Jiang, L. Zhang, J. Lu, et al., Angew. Chem. Int. Ed. 55 (2016) 7231–7235.
[18] J. Tan, Q. Li, S. Meng, et al., Adv. Mater. 33 (2021) 2006781.
[19] L. Bai, N. Xue, Y. Zhao, et al., Nano Res. 11 (2018) 2034–2045.
[20] Y. Song, S. Zhu, S. Xiang, et al., Nanoscale 6 (2014) 4676–4682.
[21] B. Wang, S. Lu, Matter 5 (2022) 110–149.
[22] C. Liu, R. Cheng, J. Guo, et al., Chin. Chem. Lett. 33 (2022) 304–307.
[23] C. Wang, Y. He, Y. Xu, et al., J. Mater. Chem. A 10 (2022) 2085–2095.
[24] C. Wang, Y. He, J. Huang, et al., J. Colloid Interface Sci. 634 (2023) 221–230.
[25] B. Zhang, B. Wang, E.V. Ushakova, et al., Small 19 (2023) 2204158.
[26] D. Zhang, D. Chao, C. Yu, et al., J. Phys. Chem. Lett. 12 (2021) 8939–8946.
[27] X. Miao, D. Qu, D. Yang, et al., Adv. Mater. 30 (2018) 1704740.
[28] C. Wang, Y. Chen, T. Hu, et al., Nanoscale 11 (2019) 11967–11974.
[29] X. Xu, L. Mo, W. Li, et al., Chin. Chem. Lett. 32 (2021) 3927–3930.
[30] P. Long, Y. Feng, C. Cao, et al., Adv. Funct. Mater. 28 (2018) 1800791.
[31] S. Wu, W. Li, W. Zhou, et al., Adv. Opt. Mater. 6 (2018) 1701150.
[32] Q. Su, C. Lu, X. Yang, Carbon 152 (2019) 609–615.
[33] Y. Ding, X. Wang, M. Tang, et al., Adv. Sci. 9 (2022) 2103833.
[34] T. Hu, Z. Wen, C. Wang, et al., Nanoscale Adv. 1 (2019) 1413–1420.
[35] S. Tao, Y. Song, S. Zhu, et al., Polymer 116 (2017) 472–478.
[36] Y. Ru, L.Z. Sui, H.Q. Song, et al., Angew. Chem. Int. Ed. 133 (2021) 14210–14218.
[37] H. Ding, S. Yu, J. Wei, et al., ACS Nano 10 (2016) 484–491.
[38] Y. Xu, C. Wang, T. Wu, et al., ACS Appl. Mater. Interfaces 14 (2022) 21310–21318.
[39] N. Soni, S. Singh, S. Sharma, et al., Chem. Sci. 12 (2021) 3615–3626.
[40] H.A. Nguyen, I. Srivastava, D. Pan, et al., ACS Nano 14 (2020) 6127–6137.
[41] L. Jiang, H. Ding, S. Lu, et al., Angew. Chem. Int. Ed. 59 (2020) 9986–9991.
[42] X. Xu, L. Mo, Y. Li, et al., Adv. Mater. 33 (2021) 2104872.
[43] M.A. Sk, A. Ananthanarayanan, L. Huang, et al., J. Mater. Chem. C 2 (2014) 6954–6960.
[44] K. Holá, M. Sudolská, S. Kalytchuk, et al., ACS Nano 11 (2017) 12402–12410.
[45] J. Chen, J. Luo, M. Hu, et al., Adv. Funct. Mater. 33 (2023) 2210095.
[46] J. Yu, X. Yong, Z. Tang, et al., J. Phys. Chem. Lett. 12 (2021) 7671–7687.
[47] N.V. Tepliakov, E.V. Kundelev, P.D. Khavlyuk, et al., ACS Nano 13 (2019) 10737–10744.